Chemosphere 180 (2017) 108–116

Contents lists available at ScienceDirect

Chemosphere

journal homepage: www.elsevier.com/locate/chemosphere

Surface functionalized composite nanofibers for efficient removal of arsenic from aqueous solutions

Alaa Mohamed [a, b, d, *], T.A. Osman [c], M.S. Toprak [a], M. Muhammed [a, e], A. Uheida [a, *]

[a] Department of Materials and Nano Physics, KTH-Royal Institute of Technology, SE 16440 Stockholm, Sweden
[b] Egypt Nanotechnology Center, EGNC, Cairo University, 12613 Giza, Egypt
[c] Mechanical Design and Production Engineering Department, Cairo University, 12613 Giza, Egypt
[d] Production Engineering and Printing Technology Department, Akhbar El Yom Academy, 12655 Giza, Egypt
[e] Material Science Department, Alexandria University, 11559 Alexandria, Egypt

HIGHLIGHTS

- Inexpensive and simple fabrication route for flexible composite nanofibers systems.
- High adsorption removal efficiency was obtained compared to other reported studies.
- Stability of the fabricated composite nanofibers allowing their reuse.
- The flexibility of the nanofibers allows use in a continuous operation mode.

GRAPHICAL ABSTRACT

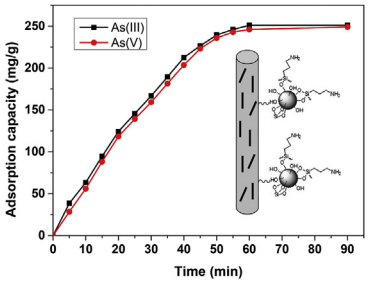

ARTICLE INFO

Article history:
Received 20 February 2017
Received in revised form
27 March 2017
Accepted 3 April 2017
Available online 4 April 2017

Handling Editor: X. Cao

Keywords:
Arsenic adsorption
Electrospinning
Isotherm
Kinetics
Composite nanofibers

ABSTRACT:

A novel composites nanofiber was synthesized based on PAN-CNT/TiO_2-NH_2 nanofibers using electrospinning technique followed by chemical modification of TiO_2 NPs. PAN-CNT/TiO_2-NH_2 nanofiber were characterized by XRD, FTIR, SEM, and TEM. The effects of various experimental parameters such as initial concentration, contact time, and solution pH on As removal were investigated. The maximum adsorption capacity at pH 2 for As(III) and As(V) is 251 mg/g and 249 mg/g, respectively, which is much higher than most of the reported adsorbents. The adsorption equilibrium reached within 20 and 60 min as the initial solution concentration increased from 10 to 100 mg/L, and the data fitted well using the linear and nonlinear pseudo first and second order model. Isotherm data fitted well to the linear and nonlinear Langmuir, Freundlich, and Redlich-Peterson isotherm adsorption model. Desorption results showed that the adsorption capacity can remain up to 70% after 5 times usage. This work provides a simple and an efficient method for removing arsenic from aqueous solution.

1. Introduction

Arsenic (As) has been recognized as one of the most toxic pollutants in an aqueous solution because of their toxicity, bioaccumulating tendency, and threat to human life and environment (Hubner et al., 2010; Sharma et al., 2014; Williams et al., 2009; Feng et al., 2013). According to the World Health Organization (WHO) the permissible maximum limit of As in drinking water is 10 μg L^{-1} (Yamamura, 2001). In an aqueous solution, arsenic exist in inorganic and organic forms as oxyanions of trivalent As(III) and pentavalent arsenic As(V). As(III) is ten times more toxic and

* Corresponding authors. Department of Materials and Nano Physics, KTH-Royal Institute of Technology, SE 16440 Stockholm, Sweden.
E-mail addresses: alakha@kth.se (A. Mohamed), salam@kth.se (A. Uheida).

http://dx.doi.org/10.1016/j.chemosphere.2017.04.011
0045-6535/

difficult to remove from aqueous solution than As(V) (Camacho et al., 2011; Boojari et al., 2016).

Due to their environmentally friendly nature, simplicity, and economy, adsorption process has been recognized as one of the most efficient techniques used for removal arsenic species from aqueous solution. Recently, many researchers have demonstrated that TiO_2 nanoparticles is effective for removal As(III) and As(V) from aqueous solutions for they easily self-aggregate in aqueous solution, which results in a fast reduction of active surface area (Niu et al., 2009; Xu and Meng, 2009; Jegadeesan et al., 2010; Pirilä et al., 2011; Guan et al., 2012; Vu et al., 2013a). Moreover, it is difficult to separate TiO_2 nanoparticles from aqueous solution after adsorption. Therefore, its need to develop an efficient technique for the removal of arsenic from contaminated water. In this regard, composite nanofibers are expected to solve these problems because they combine the advantages of nanomaterials (high specific surface area) and thin film (easy separation from water) (Mohamed et al., 2016a, 2016b). Polyacrylonitrile (PAN) has been recently used as support matrices for nanomaterials due to its excellent characteristics and commercial availability, as well as its non-toxic nature (Avila et al., 2014; Sugunan et al., 2010; Vu et al., 2013b).

In this work a novel technique has been developed to fabricate PAN-CNT/TiO_2-NH_2 nanofiber via electrospinning process using the PAN nanofibers as support matrix followed by further crosslinking of surface amino-modified TiO_2 NPs to PAN/CNT nanofibrous matrices in order to increase the adsorption of arsenic due to the large number of binding active sites incorporated on the surface of TiO_2 NPs. The effects of contact time, initial concentration, solution pH, adsorption kinetics, and isotherms were investigated. Finally, the mechanism for the removal of As using PAN-CNTs/TiO_2 has been explored.

2. Experimental

2.1. Materials

Carbon nanotubes (CNTs) with diameter between 10 and 40 nm and length 20 μm, was synthesis and the procedure is described elsewhere (Mohamed et al., 2014; Bahaa et al., 2016). Sodium arsenite ($NaAsO_2$), and sodium arsenate ($Na_3AsO_4 \cdot 12H_2O$), Polyacrylonitrile, PAN (MW = 150,000); hydroxylamine hydrochloride ($NH_2OH \cdot HCl$), sodium carbonate (Na_2CO_3), *N*, *N*-dimethylformamide (DMF), sodium hydroxide (NaOH), hydrochloric acid (HCl), titanium dioxide particulate powder (Degussa P-25), and 3-aminopropyltriethoxysilane (APTES), were purchased from Sigma Aldrich. All reagents and solvents were of analytical reagent grade and used without further purification.

2.2. Preparation of PAN-CNT/TiO_2-NH_2 composites nanofibers

CNTs were oxidized by refluxing at 120 °C in mixed acid (H_2SO_4:HNO_3 = 3:1) for 30 min and then the mixture was diluted with water and filtered. The obtained samples were washed with water and dried in the oven at 60 °C for 12 h (Khalil et al., 2016; Bahaa et al., 2017). Solution of PAN in DMF (10 wt%) was prepared and stirred for 4 h. Functionalized CNTs 3 wt% were dispersed in DMF; the dispersion was stirred for 15 min, and then sonicated for 30 min. A PAN solution was then added to the CNTs. The resulting mixture was stirred for 15 min and then sonicated for 2 h. The applied voltage was 25 kV and the distance from the tip to the collector was 15 cm. The feeding rate of the mixture solution was 0.5 mL/h.

After that the electrospun PAN-CNT nanofibers were dried in vacuum overnight to remove the excess amount of solvent. The fabrication of PAN-CNT nanofibers functionalized with amino groups was described elsewhere (Mohamed et al., 2016a). The nanofibers were placed into 100 mL solution containing a mixture of 8 g hydroxylamine hydrochloride, and 6 g of sodium carbonate. The solution and the prepared PAN-CNT nanofibers were heated to 40 °C for 6 h. The nanofibers were then washed three times with distilled water in order to remove the remaining salts and were dried in air. The surface functionalization of TiO_2 nanoparticles with the amino group was carried out according to a well established procedure (Xiang et al., 2012). Typically, 0.5 g of TiO_2 was first immersed in 10 mL of deionized water, of which pH value was adjusted to 11 by sodium hydroxide, to facilitate the adsorption of the hydroxyl group. The hydroxyl group rich TiO_2 NPs were washed twice with 20 mL of methanol to remove the excessive sodium hydroxide, and then dried in a vacuum oven at room temperature for use. Subsequent TiO_2 NPs was dispersed in 100 mL of toluene via Ultrasonication for 30 min. After that, 3 mL of silane coupling agents was added to the TiO_2 suspension. The suspension was further refluxed at 110 °C for 24 h leading to NH_2 functional group on the titania surface. The reaction product was centrifuged and washed three times with water followed by methanol to remove the unreacted silane coupling agents, and then dried in a vacuum oven prior to use. The crosslinking of the amino functionalized composite nanofibers (PAN-CNT-NH_2) to TiO_2-NH_2 via the amine side was carried out as follow: PAN-CNT-NH_2 composite nanofibers weighted and immersed in the crosslinking medium containing 2.5 wt% Glutaraldehyde (GA), and kept shaking for 24 h at room temperature. After the activation reaction of the composite nanofibers was completed, the GA crosslinking medium was removed and then 2 mL of an aqueous dispersion of functionalized TiO_2 nanoparticles was added to the composite nanofibers for 24 h. The crosslinked composite nanofibers were washed with ethanol followed by distilled water to remove the excess of non-crosslinked nanoparticles and then the composite nanofibers were dried in air at room temperature.

2.3. Adsorption of As

The Adsorption of As in an aqueous solution was carried out in a 100 mL quartz reactor containing 25 mg composite nanofibers and 50 mL 10 ppm of As (III) and As (V). The composite nanofibers were dispersed in As solution under shaking condition at room temperature, then 3 mL of the suspension was taken from the reactor at a scheduled interval. The concentration of arsenic was measured using a Inductively Coupled Plasma Optical Emission Spectroscopy (ICP-OES) (Thermo Fisher iCAP 6500). The pH values of the solution were adjusted by adding 0.1 M NaOH or 0.1 M HNO_3 and was varied within the range of 2–9. The equilibrium adsorption capacity (q_e) was determined using equation (1), while % removal of As (III) and As (V) was calculated using equation (2).

$$q_e = \frac{(C_0 - C_e)V}{m} \tag{1}$$

$$(\%)\text{Removal} = \left(\frac{C_0 - C_e}{C_0}\right) \times 100 \tag{2}$$

where, C_0 is the initial arsenic concentration (mg/L) and C_e is the arsenic concentration in the aqueous solution at equilibrium (mg/L), V is the total aqueous volume (L), and m is the mass of the composite nanofibers (g).

2.4. Characterization

The morphology of PAN and PAN-CNT/TiO_2-NH_2 composites nanofiber functionalized membranes was characterized using field

emission scanning electron microscopy (FE-SEM, Gemini Zeiss-Ultra 55), and transmission electron microscopy (TEM, JEM-2100F, Joel). The functional groups on the surface of synthesized nanofiber were characterized using a Nicolet Nexus iS10 FT-IR to confirm the presence of amino groups on the surface of the nanoparticles as well as covalent attachment of nanoparticles on the surface of the nanofibers. The phase structure of the composites nanofiber was characterized by X-ray diffraction (XRD, Bruker AXS D8 Advance diffractometer operating with Cu-Kα radiation) in the scan range 2θ between 10° and 70°.

3. Results and discussions

3.1. Characterization of materials

The morphologies of PAN and PAN-CNT/TiO_2-NH_2 nanofibers are observed by SEM, and TEM, the results are shown in Fig. 1. It can be seen that the nanofibers are composed of numerous, randomly oriented nanofibers, and the pure PAN nanofibers are smooth and uniform, with average diameters is about 120 nm (Fig. 1a). After the chemical modification on the surface of PAN nanofibers, the average diameter increased to 210 nm (Fig. 1b), and the surface of the PAN-CNT/TiO_2-NH_2 nanofibers became more coarse than the pure PAN. Fig. 1c shows TEM images of the PAN-CNT/TiO_2-NH_2 nanofibers. It is obvious that composite nanofibers are composed of TiO_2 nanoparticles, aggregated along fiber orientation.

The crystal phase structure of the PAN-CNT/TiO_2-NH_2 nanofibers was characterized by XRD measurement as shown in Fig. 2a. The XRD patterns of the PAN-CNT/TiO_2-NH_2 nanofibers show maximum diffraction peaks at $2\theta = 16.8°$ and 28.6° represented the crystallographic planes in PAN. In addition, the FTIR spectrum of PAN nanofiber (Fig. 2b) exhibited the absorption peaks of a stretching vibration at 2243 cm^{-1} (C≡N), 1732 cm^{-1} (C═O), and 1452 cm^{-1} (C–O), which suggests that the PAN was a copolymer of acrylonitrile and methylacrylate (Saeed et al., 2008). The FTIR spectrum of PAN-CNT/TiO_2-NH_2 nanofiber shows the absorption peak at 3170–3500 cm^{-1} and 1668 cm^{-1} corresponding to stretching vibrations of the –OH and bending vibrations of the adsorbed water molecules respectively. The transmittance peak at 1620 and 1452 cm^{-1} were assigned to the (NH_2) group and the absorption bands at 1454, 1102, and 908 cm^{-1} were assigned to the C-H, C-C, and N-O, respectively (Mohamed et al., 2016a; Yousef and Mohamed, 2016).

3.2. Effect of pH on adsorption of As

The pH value of solution played an important role in the adsorption because pH value can not only have an effect on the surface state of the adsorbent but also on the existing form of the adsorbate. The effect of pH solution on adsorption of As(III) and As(V) using PAN-CNT/TiO_2-NH_2 nanofibers under pH value from 2 to 9, are presented in Fig. 3. The maximum adsorption removal for As(III) and As(V) was observed at pH 2. The extent of As(III) removal was 99.9–72% in the pH range 2–9, while 99.2%–55% for As(V) in the same pH range. Thus, the PAN-CNT/TiO_2-NH_2 can be considered as a highly efficient adsorbent for the removal of both As(III) and As(V) in acidic and neutral pH range, which is similar to a previous report (Miller et al., 2011; Kanel et al., 2005; Gupta and Ghosh, 2009; Polowczyk et al., 2016; Iervolino et al., 2016; Wei et al., 2016; Yu et al., 2006). This may be due to the electrostatic interaction

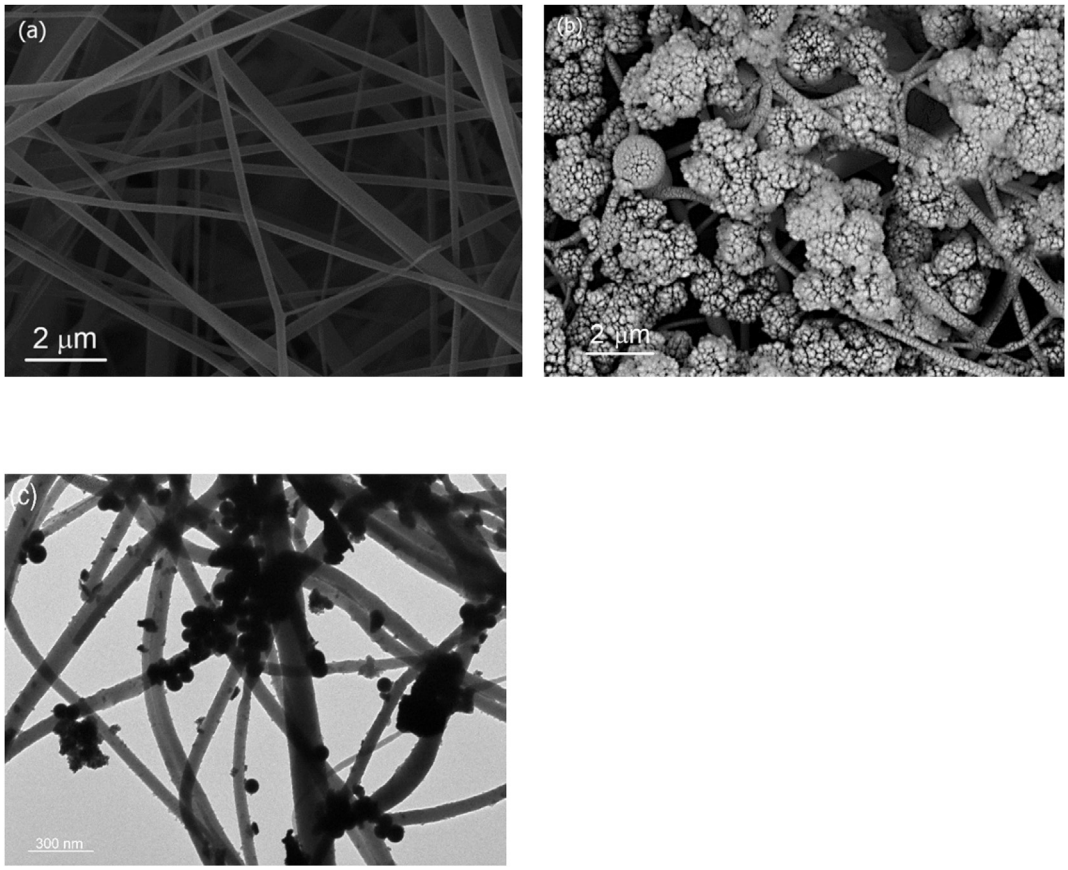

Fig. 1. FE-SEM images of (a) PAN nanofibers, (b) PAN-CNT/TiO_2-NH_2, and (c) TEM image of PAN-CNT/TiO_2-NH_2.

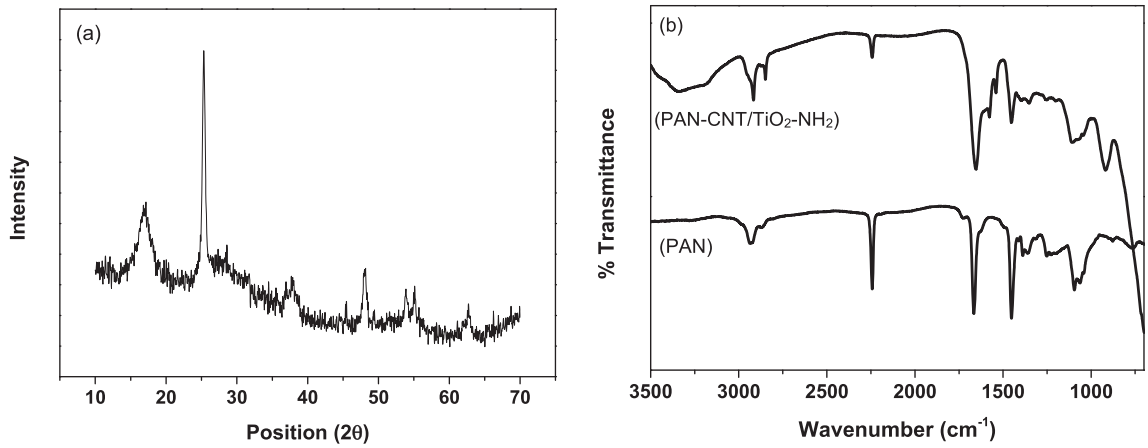

Fig. 2. (a) XRD patterns and (b) FTIR spectrum of the PAN-CNT/TiO_2-NH_2.

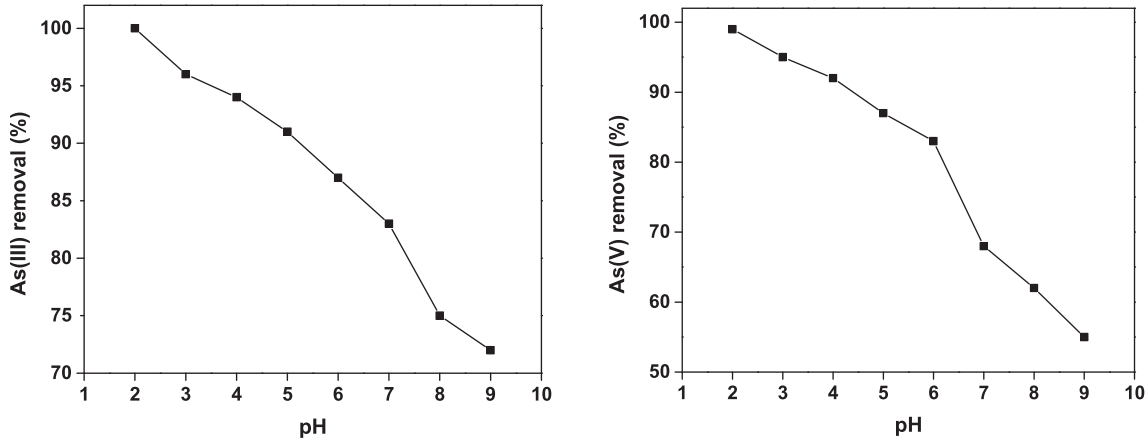

Fig. 3. (a) Effect of pH solution on the removal of (a) As(III) and (b) As(V) using PAN-CNT/TiO_2-NH_2 nanofibers (As(III) = 10 ppm, As(V) = 10 ppm).

between positively charged amine groups and negatively charged of As(III) and As(V) species (Anđelković et al., 2016; Yamani et al., 2014; Giasuddin et al., 2007). In addition due to the electrostatic attraction and complexation between positively charged surface hydroxyl group and As (Amiri et al., 2004; Mandal et al., 2013).

3.3. Kinetics of As adsorption

Adsorption kinetics is one of the most important parameters for describing the adsorption efficiency. Kinetics adsorption is performed to evaluate the equilibrium time at different concentration on the adsorption capacity of As(III) and As(V) as shown in Fig. 4. It demonstrated that the As(III) and As(V) adsorption capacity of PAN-CNT/TiO_2-NH_2 increases gradually with increasing the concentrations until an equilibrium was established. The removal of As(III) and As(V) occurred rapidly and reached adsorption equilibrium within 25 min for 10 ppm, while for 100 ppm take 1 h to reach adsorption equilibrium, and after that the adsorption of As(III) and As(V) becomes stagnant. It is further observed that maximum adsorption capacity of As(III) and As(V) is 250 mg/g. This phenomenon may be due the electrostatic interaction between the positive protonated amidine, amine groups and negative As(III) and As(V) ions and the high density of active sites of PAN-CNT/TiO_2-NH_2 nanofiber (Chauhan et al., 2014). Therefore, the adsorption process was very fast at short adsorption equilibrium time. Two kinetic models, linear and non linear pseudo-first-order and pseudo-second-order, expressed by Eqs. (3)–(6) respectively, are utilized to fit the experimental data and evaluate the adsorption kinetic process (Min et al., 2015; Mahanta and Valiyaveettil, 2013; Morillo et al., 2015; Bhaumik et al., 2015).

$$\log(q_e - q_t) = \log\ q_e\ - \frac{K_1}{2.303}t \tag{3}$$

$$\frac{t}{q_t} = \frac{1}{k_2 q_e^2} + \frac{1}{q_e}t \tag{4}$$

$$q_t = q_e\left(1 - e^{-k_3 t}\right) \tag{5}$$

$$q_t = \frac{k_2 q_e^2 \mathrm{t}}{1 + k_4 q_e \mathrm{t}} \tag{6}$$

where q_e and q_t are the adsorption capacities of As(III) and As(V) (mg/g) at equilibrium time and at any instant of time t (min), respectively. Where K_1 and K_2 are the linear pseudo first order and second order rate constants, respectively. K_3 and k_4 are the rate constant of non linear pseudo-first order adsorption (1/min), and pseudo-second order (g/mg min). The linear and nonlinear plots of pseudo first order kinetic and pseudo second order kinetic models for both As species are shown in Figs. 5–7. The obtained kinetic parameters of linear pseudo-first-order and pseudo second order

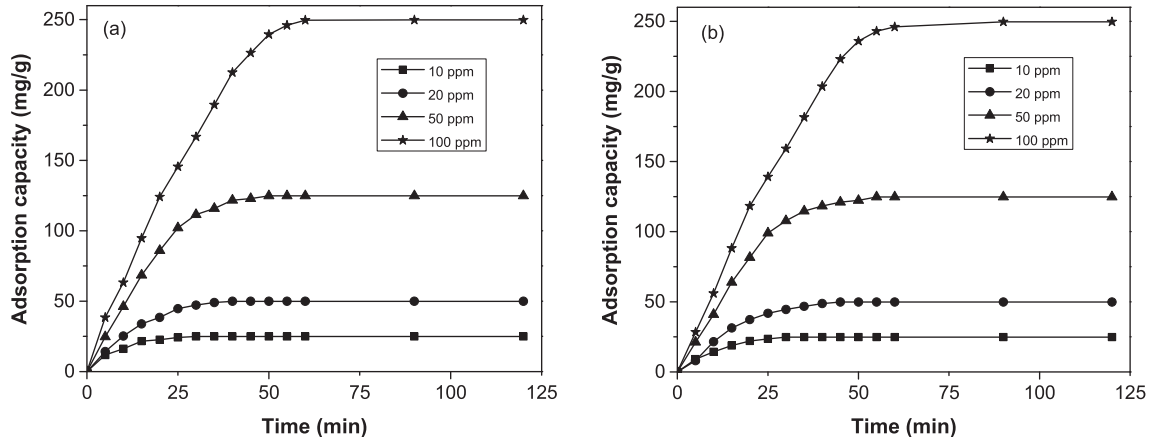

Fig. 4. Effect of time on the adsorption capacity of (a) As(III) and (b) As(V).

for As(III) and As(V) are summarized in Table 1. The correlation coefficient (R^2) for the pseudo second order kinetics model is higher than that for the pseudo first order kinetics model indicated that the adsorption kinetics closely followed the pseudo second order model rather than the pseudo first order model. Furthermore, the parameters of nonlinear pseudo-first-order and pseudo-second-order kinetic models for As(III) and As(V) are summarized in Table 1. It should be observed that the q_e values obtained from the pseudo first order model are close to experimental q_{exp} for As(III) and As(V). These results confirm that As(III) and As(V) adsorption kinetics are better described by the pseudo first order mechanism.

3.4. Adsorption isotherms of As

Adsorption isotherms are commonly used to calculate the

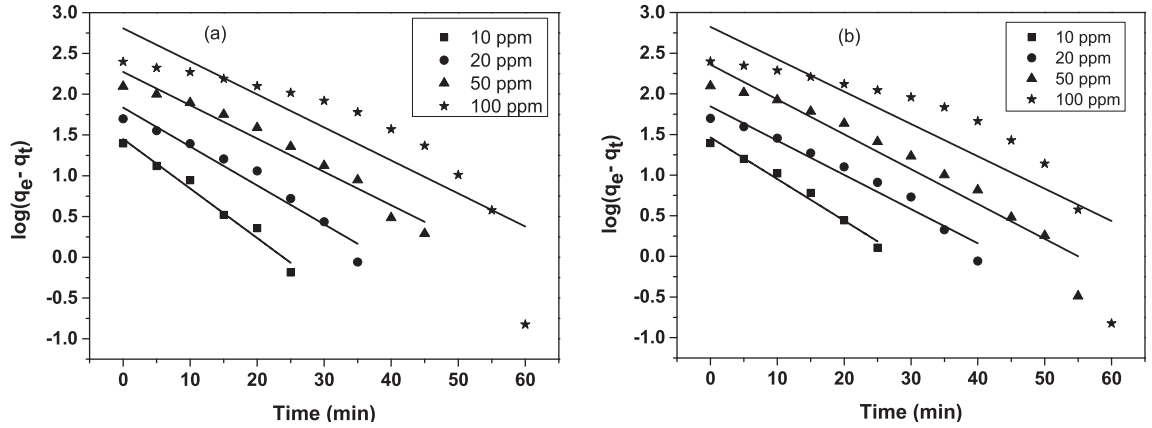

Fig. 5. Linear Pseudo first order for adsorption of a) As(III) b) As(V) using PAN-CNT/TiO_2-NH_2 nanofibers (pH = 2).

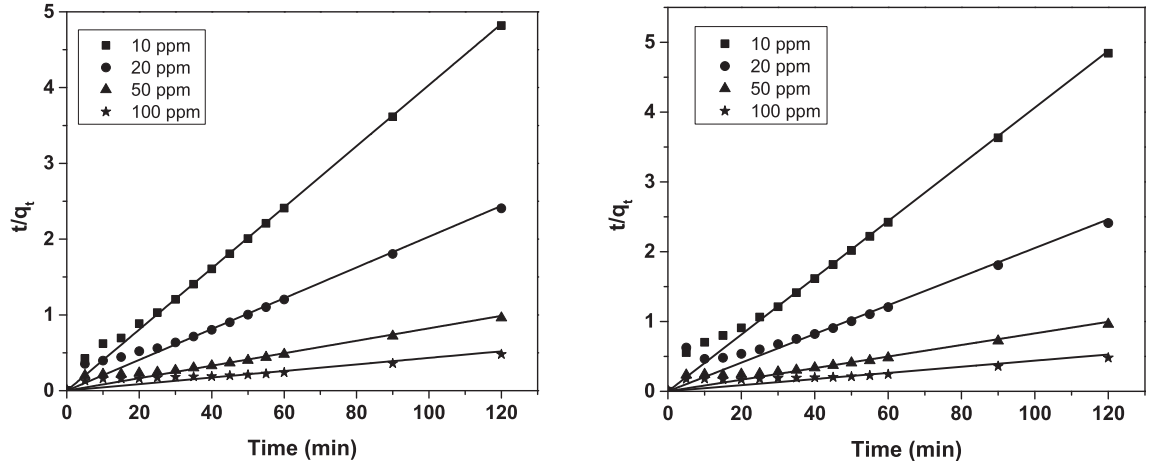

Fig. 6. Linear Pseudo second order for adsorption of a) As(III) b) As(V) using PAN-CNT/TiO_2-NH_2 nanofibers (pH = 2).

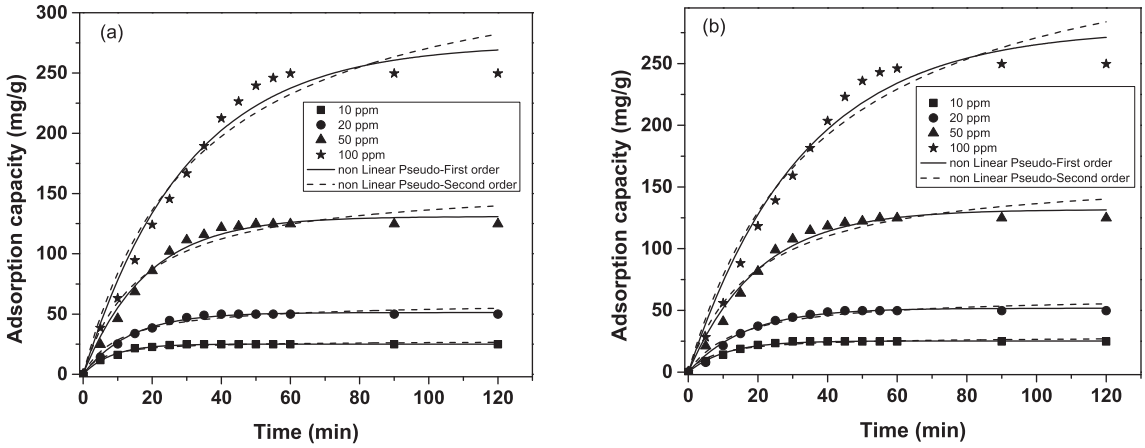

Fig. 7. Non-linear first-order and Second-order plot for the adsorption of a) As(III) b) As(V) using PAN-CNT/TiO_2-NH_2 nanofibers (pH = 2).

Table 1
Kinetics parameters for As(III) and As(V) adsorption using PAN-CNT/TiO_2-NH_2 nanofiber.

	Parameters	As(III)				As(V)			
C_0 (mg/L)		10	20	50	100	10	20	50	100
$q_{e,exp}$ (mg/g)		24.9	49.9	124.8	251.2	24.78	49.8	124.8	249.6
Linear Pseudo first order model	K_1 (1/min)	−0.061	−0.048	−0.041	−0.041	−0.051	−0.042	−0.043	−0.040
	$q_{e,cal}$ (mg/g)	10.6	119.5	1242.9	6527.8	21.1	180	1319.8	7102.9
	R^2	0.967	0.945	0.957	0.737	0.975	0.950	0.931	0.708
Linear Pseudo second order model	K_2 (g/mg min)	0.004	0.008	0.02	0.04	0.0044	0.008	0.021	0.041
	$q_{e,cal}$ (mg/g)	24.2	18.8	15.7	13.9	20.2	14.1	14.2	11.8
	R^2	0.931	0.975	0.991	0.998	0.904	0.966	0.974	0.996
Non Linear Pseudo first order model	q_e (mg/g)	25.15	51.24	130.97	274.06	25.237	51.75	131.70	278.13
	K_3 (1/min)	0.119	0.074	0.055	0.003	0.093	0.062	0.050	0.0031
	R^2	0.995	0.994	0.985	0.978	0.994	0.990	0.982	0.973
Non Linear Pseudo second order model	q_e (mg/g)	27.75	59.76	159.14	359.6	28.65	61.79	162.4	372.3
	K_4 (g/mg min)	0.0066	0.0015	3.78E-4	8.47E-5	0.0045	0.0012	3.25E-4	7.17E-5
	R^2	0.972	0.964	0.952	0.955	0.962	0.959	0.950	0.951

maximum adsorption capacity of PAN-CNT/TiO_2-NH_2 nanofiber for the As(III) and As(V) by studying the interactions between adsorbate and an adsorbent. The adsorption experimental data were fitted with three commonly used isotherm models, linear and nonlinear Langmuir, Freundlich, and Redlich-Peterson equation, expressed by Eqs. (7)–(11), and (10), respectively (Foo and Hameed, 2010; Zhang et al., 2010; Brdar et al., 2012). Langmuir isotherm is mainly applied to describe the monolayer adsorption on perfectly smooth and homogeneous surface of adsorbent.

$$\frac{C_e}{q_e} = \frac{1}{q_m K_a} + \frac{C_e}{q_m} \tag{7}$$

$$q_e = \frac{q_m K_a C_e}{1 + K_a C_e} \tag{8}$$

where q_m (mg/g) is the maximum adsorption capacity and k_a (L/mg) is the Langmuir constant related to the energy of adsorption, and C_e is the equilibrium concentration (mg/L).

The Freundlich isotherm is commonly used to describe the multilayer adsorption on a heterogeneous surface with a nonuniform distribution of the heat of sorption over the surface. The Freundlich model is expressed as:

$$log\ q_e = log\ K_F + \frac{1}{n} \log C_e \tag{9}$$

$$q_e = K_F\, C_e^{1/n} \tag{10}$$

where K_F and 1/n are Freundlich constants related to the adsorption capacity (mg/g) and intensity of adsorption, respectively.

The Redlich-Peterson isotherm contains three parameters, K_R, α_R and g, and incorporates the features of the Langmuir and the Freundlich isotherms (Gogoi et al., 2016). It may be used to represent adsorption equilibrium over a wide concentration range of adsorbate. The exponent, g, lies between 0 and 1. When g = 1, the Redlich–Peterson equation becomes the Langmuir equation, and when g = 0, it becomes the Henry's law. This isotherm is described as follows:

$$\ln\left(K_R \frac{C_e}{q_e} - 1\right) = g \ln(C_e) + \ln(\alpha_R) \tag{11}$$

$$q_e = \frac{K_R C_e}{1 + \alpha_R C_e^g} \tag{12}$$

where K_R, α_R, and g ($0 < g < 1$), are three isotherm constants.

The linear and nonlinear Langmuir, Freundlich, and Redlich-Peterson isotherm plots are presented in Figs. 8 and 9. It can be observed that the PAN-CNT/TiO_2-NH_2 have high sorption capacity for both As(III) and As(V). Table 2 summarizes the linear and nonlinear Langmuir, Freundlich, and Redlich-Peterson isotherm parameters for As(III) and As(V) adsorption by the PAN-CNT/TiO_2-

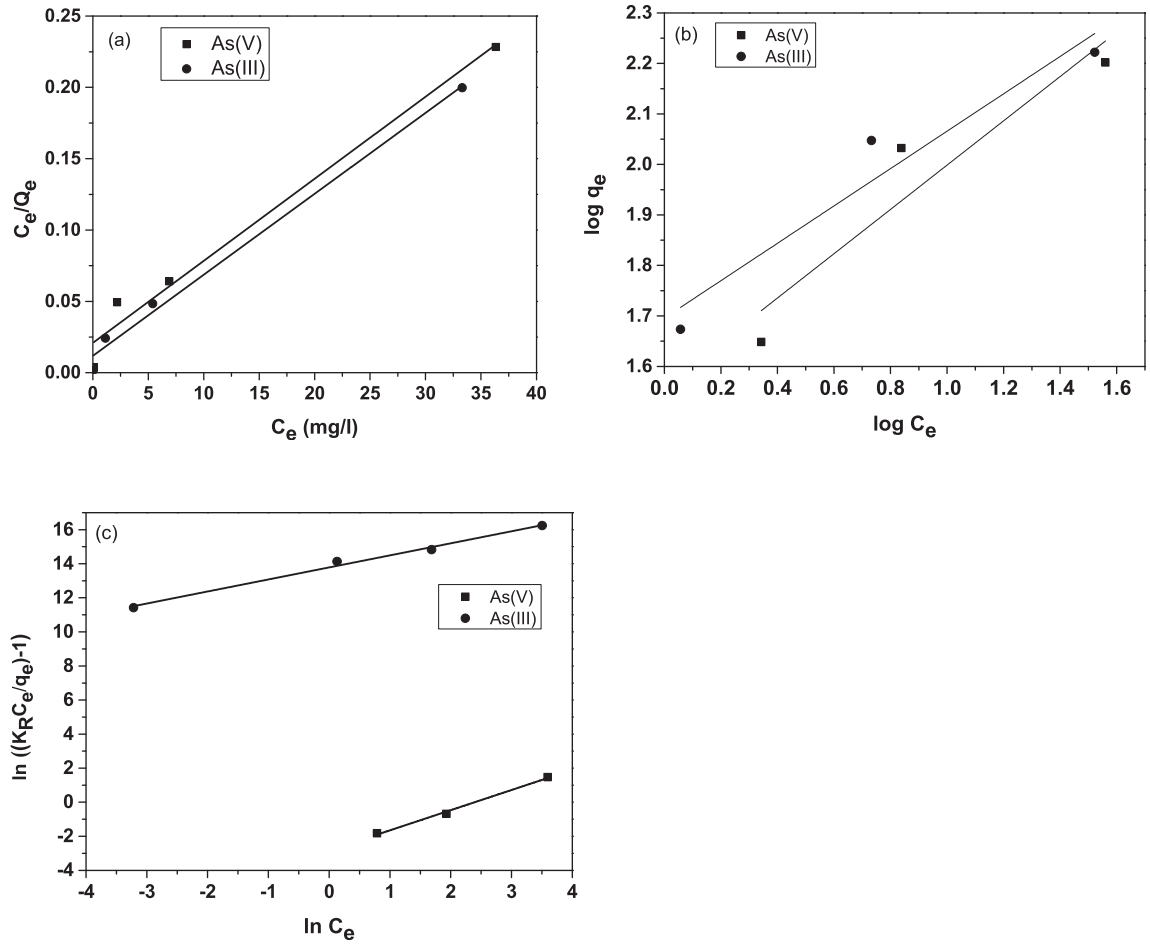

Fig. 8. a) Linear Langmuir isotherm model, b) Freundlich isotherm model, c) Redlich-Peterson isotherm model for adsorption of As(III) and As(V) using PAN-CNT/TiO_2-NH_2 nanofibers.

NH_2. The very high values of correlation coefficients (R^2) reveal that the Langmuir model fitted well the isotherm data better than the Freundlich model, and Redlich-Peterson. Thus, monolayer adsorption happened on the adsorbents. The Langmuir maximum adsorption capacities (q_m) of PAN-CNT/TiO_2-NH_2 for As(III) and As(V), as estimated from the linear and non-linear Langmuir isotherm plots are 227.27 and 225.87 mg/g for As(V), and 232.55 and 228.94 mg/g for As(III). The maximum As adsorption capacity of the PAN-CNT/TiO_2-NH_2 nanofibers is mainly attributed to the small size of the TiO_2 nanoparticles immobilized on the high surface area PAN-CNTs nanofibers matrix.

Table 3 lists the maximum adsorption capacities of As(III) and As(V) on PAN-CNT/TiO_2-NH_2 and other TiO_2 related adsorbents reported in the literature. The data indicates that the PAN-CNT/

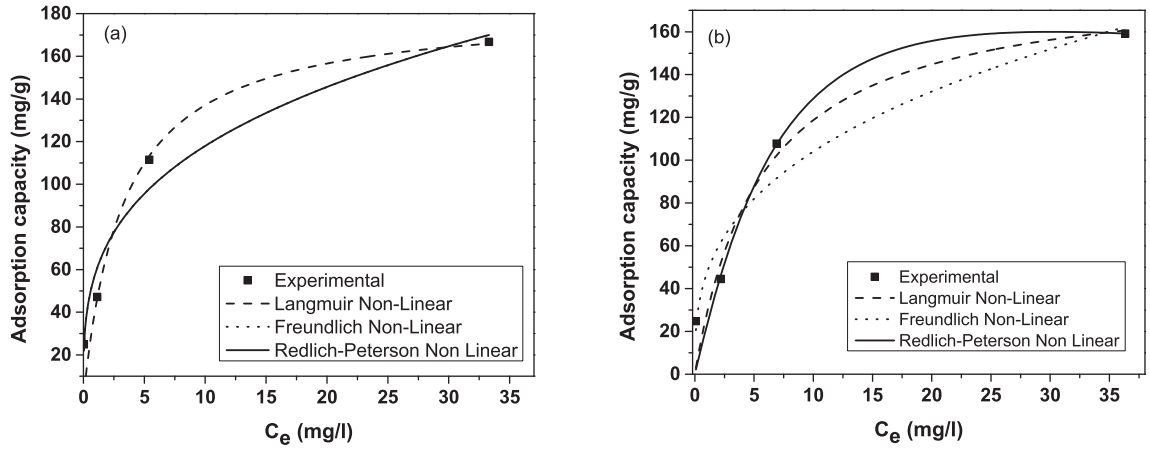

Fig. 9. Nonlinear Langmuir isotherm model, Freundlich isotherm model, Redlich-Peterson isotherm model for adsorption of a) As(III) b) As(V) using PAN-CNT/TiO_2-NH_2 nanofibers.

Table 2
Langmuir, Freundlich and Redlich-Peterson isotherm parameters for As(V) and As(III) adsorption onto PAN-CNT/TiO_2-NH_2 composites nanofiber

	Parameters	As(III)	As(V)
Linear Langmuir isotherm model	K_a (L/mg)	0.006	0.006
	q_m (mg/g)	887.5	803.4
	R^2	0.99	0.97
Linear Freundlich isotherm model	K_F (mg/g)	0.37	0.44
	n	2.893	2.432
	R^2	0.876	0.79
Linear Redlich-Peterson isotherm model	K_R (L $mg^{1-1/A}$)	4.32	4.33
	α_R	341229.4	0.12
	g	0.828	0.952
	R^2	0.988	0.99
Non Linear Langmuir isotherm model	K_a (L/mg)	0.303	0.17783
	q_m (mg/g)	182.47	185.459
	R^2	0.937	0.924
Non Linear Freundlich isotherm model	K_F (mg/g)	58.623	47.06
	n	3.29	2.903
	R^2	0.952	0.923
Non Linear Redlich-Peterson isotherm model	K_R (L $mg^{1-1/A}$)	5.69 E7	23.505
	α_R	971114.1	0.04217
	g	0.696	1.2914
	R^2	0.904	0.862

Table 3
Comparison of maximum As adsorption capacities (mg/g) of PAN-CNT/TiO_2-NH_2 related adsorbents.

Adsorbent	pH	q_{max} (mg/g)		concentration of As (mg/L)	Equilibrium time (min)	Ref.
		As(III)	As(V)			
PVP/TiO_2 NFs	7	0.045 mmol/g		0.0133 mmol/kg	210	(Vu et al., 2013a)
Ce–Ti oxide	6.5	6.8	7.5	0.01	720	(Li et al., 2010)
CS-ENM	4.4	–	30.8	2	30	(Min et al., 2015)
CTAB/TiO_2	7	–	1.024	0.01	90	(Gogoi et al., 2016)
Granular TiO_2	7	32.4	41.4	0.3	240	(Bang et al., 2005)
Titanate nanotubes	3	60	208	5	720	(Niu et al., 2009)
Fe_3O_4/TiO_2–SiO_2	7	24	–	10	300	(Sadeghi et al., 2016)
TiO_2 NPs	7	30	30.5	50	240	(Xu and Meng, 2009)
PAN-CNT/TiO_2-NH_2 NFs	2	251	249	10	60	This work

TiO_2-NH_2 adsorbent shows higher adsorption capacity than many other reported TiO_2 adsorbents. Therefore, it's concluded that the PAN-CNT/TiO_2-NH_2 nanofibers could be used as an effective adsorbent for adsorption of As(III) and As(V) in aqueous solution. TiO_2 has proven to be effective for As(III) and As(V) removal due to the presence of high affinity surface hydroxyl groups on the TiO_2 surface, which can form the surface complexes with As(III) and As(V) (Guan et al., 2012). Thus, it can be concluded that PAN-CNT/TiO_2-NH_2 nanofibers are very promising materials for As(III) and As(V) removal from aqueous solution.

3.5. Regeneration and reusability of PAN-CNT/TiO_2-NH_2 nanofiber

Regenerate and rues of the adsorbent material are an important factors in wastewater treatment processes for evaluating the cost effectiveness. To check the regeneration and reusability of PAN-CNT/TiO_2-NH_2 nanofiber for As removal, five consecutive adsorption–desorption cycles were carried out. The regenerated nanofiber showed good reusability in the first three cycles for As(III) and As(V). It was observed that in the first desorption cycle, the removal percentage of As(III) and As(V) was found to be 97 and 99%, respectively. In second cycle, approximately 4% decrement was observed for both arsenic species and in subsequent cycles only 7% change was observed. However, the removal percentage was declined gradually after three adsorption-desorption cycles, which may be attributed to the deformation of nanofibers in NaOH medium during regeneration. However, the decrease in the removal percentage was not substantial. These results indicate that the PAN-CNT/TiO_2-NH_2 nanofiber could be regenerated upon NaOH treatment and may be reused for further As removal up to five cycles (70% removal).

4. Conclusions

Novel PAN-CNT/TiO_2-NH_2 nanofibers were prepared by electrospinning technique and they were further modified with crosslinking of TiO_2 NPs onto the PAN-CNT nanofibers matrix for the effective adsorption of As from aqueous solution. Experimental results demonstrated that PAN-CNT/TiO_2-NH_2 are very effective in removing As(III) and As(V) with high maximum adsorption capacities of 251 and 249 mg/g, respectively, at pH 2.0. The adsorption kinetics fitted well with nonlinear pseudo second-order kinetic model, and the adsorption isotherms data are well-fitted with nonlinear Langmuir isotherm model. Moreover, regeneration studies revealed that the adsorption capacities of the adsorbent for both As(III) and As(V) were slightly decreased. Therefore, PAN-CNT/TiO_2-NH_2 nanofibers, could be applied as a promising adsorbent because it have high adsorption capacity, and fast adsorption rate, which were favorable for the treatment of drinking water/groundwater contaminated by As.

References

Amiri, F., et al., 2004. Sorption behaviour of phenols on natural sandy aquifer material during flow-through column experiments: the effect of pH. Acta Hydrochim Hydrobiol 32 (3), 214–224.
Anđelković, I., et al., 2016. Investigation of mechanism and critical parameters for removal of arsenic from water using Zr-TiO2 composite. Environ. Technol. 1–23.
Avila, M., et al., 2014. Surface functionalized nanofibers for the removal of

chromium(VI) from aqueous solutions. Chem. Eng. J. 245, 201–209.
Kamel, Bahaa M., Mohamed, A., El Sherbiny, M., Abed, K.A., 2016. Tribological behaviour of calcium grease containing carbon nanotubes additives. Ind. Lubr. Tribol. 68 (6), 723–728.
Bahaa, M. Kamel, Alaa Mohamed, El Sherbiny, M., Abed, K.A., Abd-Rabou, M., 2017. Tribological properties of graphene nanosheets as an additive in calcium grease. J. Dispers. Sci. Technol. 38 (10).
Bang, S., et al., 2005. Removal of arsenic from groundwater by granular titanium dioxide adsorbent. Chemosphere 60 (3), 389–397.
Bhaumik, M., et al., 2015. Polyaniline/Fe0 composite nanofibers: an excellent adsorbent for the removal of arsenic from aqueous solutions. Chem. Eng. J. 271, 135–146.
Boojari, H., Pourafshari Chenar, M., Pakizeh, M., 2016. Experimental investigation of arsenic (III, V) removal from aqueous solution using synthesized α-Fe2O3/MCM-41 nanocomposite adsorbent. Water Air Soil Pollut. 227 (8), 290.
Brdar, M., et al., 2012. Comparison of two and three parameters adsorption isotherm for Cr(VI) onto Kraft lignin. Chem. Eng. J. 183, 108–111.
Camacho, L.M., et al., 2011. Occurrence and treatment of arsenic in groundwater and soil in northern Mexico and southwestern USA. Chemosphere 83 (3), 211–225.
Chauhan, D., Dwivedi, J., Sankararamakrishnan, N., 2014. Novel chitosan/PVA/zerovalent iron biopolymeric nanofibers with enhanced arsenic removal applications. Environ. Sci. Pollut. Res. 21 (15), 9430–9442.
Feng, Q., et al., 2013. Adsorption and desorption characteristics of arsenic on soils: kinetics, equilibrium, and effect of Fe(OH)3 colloid, H2SiO3 colloid and phosphate. Proc. Environ. Sci. 18, 26–36.
Foo, K.Y., Hameed, B.H., 2010. Insights into the modeling of adsorption isotherm systems. Chem. Eng. J. 156 (1), 2–10.
Giasuddin, A.B.M., Kanel, S.R., Choi, H., 2007. Adsorption of humic acid onto nanoscale zerovalent iron and its effect on arsenic removal. Environ. Sci. Technol. 41 (6), 2022–2027.
Gogoi, P., Dutta, Debasish, Maji, T.K., 2016. Equilibrium and kinetics study on removal of arsenate ions from aqueous solution by CTAB/TiO_2 and starch/CTAB/TiO_2 nanoparticles: a comparative study. J. Water Health (5).
Guan, X., et al., 2012. Application of titanium dioxide in arsenic removal from water: a review. J. Hazard. Mater. 215–216, 1–16.
Gupta, K., Ghosh, U.C., 2009. Arsenic removal using hydrous nanostructure iron(-III)–titanium(IV) binary mixed oxide from aqueous solution. J. Hazard. Mater. 161 (2–3), 884–892.
Hubner, R., Astin, K.B., Herbert, R.J.H., 2010. 'Heavy metal'-time to move on from semantics to pragmatics? J. Environ. Monit. 12 (8), 1511–1514.
Iervolino, G., et al., 2016. Removal of arsenic from drinking water by photo-catalytic oxidation on MoOx/TiO2 and adsorption on γ-Al2O3. J. Chem. Technol. Biotechnol. 91 (1), 88–95.
Jegadeesan, G., et al., 2010. Arsenic sorption on TiO2 nanoparticles: size and crystallinity effects. Water Res. 44 (3), 965–973.
Kanel, S.R., et al., 2005. Removal of arsenic(III) from groundwater by nanoscale zero-valent iron. Environ. Sci. Technol. 39 (5), 1291–1298.
Khalil, Waleed, Mohamed, A., Bayoumi, Mohamed, Osman, T.A., 2016. Tribological properties of dispersed carbon nanotubes in lubricant. Fullerenes. Nanotub. Carbon Nanostruct. 24 (7), 479–485.
Li, Z., et al., 2010. As(V) and As(III) removal from water by a Ce–Ti oxide adsorbent: behavior and mechanism. Chem. Eng. J. 161 (1–2), 106–113.
Mahanta, N., Valiyaveettil, S., 2013. Functionalized poly(vinyl alcohol) based nanofibers for the removal of arsenic from water. RSC Adv. 3 (8), 2776–2783.
Mandal, S., Sahu, M.K., Patel, R.K., 2013. Adsorption studies of arsenic(III) removal from water by zirconium polyacrylamide hybrid material (ZrPACM-43). Water Resour. Ind. 4, 51–67.
Miller, S.M., Spaulding, M.L., Zimmerman, J.B., 2011. Optimization of capacity and kinetics for a novel bio-based arsenic sorbent, TiO2-impregnated chitosan bead. Water Res. 45 (17), 5745–5754.
Min, L.-L., et al., 2015. Preparation of chitosan based electrospun nanofiber membrane and its adsorptive removal of arsenate from aqueous solution. Chem. Eng. J. 267, 132–141.
Mohamed, Alaa, Osman, T.A., Khattab, Ali, Zaki, M., 2014. Tribological behavior of carbon nanotubes as an additive on lithium grease. J. Tribol. 137 (1), 011801–011801.
Mohamed, Alaa, Osman, T.A., Toprak, M.S., Muhammed, M., El-Sayed, Ramy, Uheida, A., 2016. Composite nanofibers for highly efficient photocatalytic degradation of organic dyes from contaminated water. Environ. Res. 145, 18–25.
Mohamed, Alaa, Osman, T.A., Toprak, M.S., Muhammed, M., Yilmaz, Eda, Uheida, A., 2016. Visible light photocatalytic reduction of Cr(VI) by surface modified CNT/titanium dioxide composites nanofibers. J. Mol. Catal. A Chem. 424, 45–53.
Morillo, D., et al., 2015. Arsenate removal with 3-mercaptopropanoic acid-coated superparamagnetic iron oxide nanoparticles. J. Colloid Interface Sci. 438, 227–234.
Niu, H.Y., et al., 2009. Adsorption behavior of arsenic onto protonated titanate nanotubes prepared via hydrothermal method. Microporous Mesoporous Mater. 122 (1–3), 28–35.
Pirilä, M., et al., 2011. Removal of aqueous As(III) and As(V) by hydrous titanium dioxide. J. Colloid Interface Sci. 353 (1), 257–262.
Polowczyk, I., et al., 2016. Influence of pH on arsenic(III) removal by fly ash. Sep. Sci. Technol. 51 (15–16), 2612–2619.
Sadeghi, M., et al., 2016. Removal of Arsenic (III) from natural contaminated water using magnetic nanocomposite: kinetics and isotherm studies. J. Iran. Chem. Soc. 13 (7), 1175–1188.
Saeed, K., et al., 2008. Preparation of amidoxime-modified polyacrylonitrile (PAN-oxime) nanofibers and their applications to metal ions adsorption. J. Membr. Sci. 322 (2), 400–405.
Sharma, R., et al., 2014. Electrospun chitosan-polyvinyl alcohol composite nanofibers loaded with cerium for efficient removal of arsenic from contaminated water. J. Mater. Chem. A 2 (39), 16669–16677.
Sugunan, A., et al., 2010. Radially oriented ZnO nanowires on flexible poly-l-lactide nanofibers for continuous-flow photocatalytic water purification. J. Am. Ceram. Soc. 93 (11), 3740–3744.
Vu, D., et al., 2013a. Phase-structure effects of electrospun TiO2 nanofiber membranes on as(III) adsorption. J. Chem. Eng. Data 58 (1), 71–77.
Vu, D., Li, X., Wang, C., 2013b. Efficient adsorption of As(V) on poly(acrylo-amidino ethylene amine) nanofiber membranes. Chin. Sci. Bull. 58 (14), 1702–1707.
Wei, Z., et al., 2016. The effect of pH on the adsorption of arsenic(III) and arsenic(V) at the TiO2 anatase [1 0 1] surface. J. Colloid Interface Sci. 462, 252–259.
Williams, P.N., et al., 2009. Occurrence and partitioning of cadmium, arsenic and lead in mine impacted paddy rice: Hunan, China. Environ. Sci. Technol. 43 (3), 637–642.
Xiang, C., et al., 2012. Experimental and statistical analysis of surface charge, aggregation and adsorption behaviors of surface-functionalized titanium dioxide nanoparticles in aquatic system. J. Nanopart. Res. 15 (1), 1293.
Xu, Z., Meng, X., 2009. Size effects of nanocrystalline TiO2 on As(V) and As(III) adsorption and As(III) photooxidation. J. Hazard. Mater. 168 (2–3), 747–752.
Yamamura, S., 2001. Drinking Water Guidelines and Standards. World Health Organization.
Yamani, J.S., Lounsbury, A.W., Zimmerman, J.B., 2014. Adsorption of selenite and selenate by nanocrystalline aluminum oxide, neat and impregnated in chitosan beads. Water Res. 50, 373–381.
Yousef, S., Mohamed, A., 2016. Mass production of CNTs using CVD multi-quartz tubes. J. Mech. Sci. Technol. 30 (11), 5135–5141.
Yu, J., et al., 2006. Effects of pH on the microstructures and photocatalytic activity of mesoporous nanocrystalline titania powders prepared via hydrothermal method. J. Mol. Catal. A Chem. 258 (1–2), 104–112.
Zhang, L., et al., 2010. Isotherm study of phosphorus uptake from aqueous solution using aluminum oxide. Clean – Soil Air Water 38 (9), 831–836.